International Journal of Surface Science and Engineering

ISSN online: 1749-7868 - ISSN print: 1749-785X
https://www.inderscience.com/ijsurfse

Investigation of solid particle erosion behaviour of Fe-Cr alloy coating

Ratnesh Kumar Sharma, Randip Kumar Das, Shiv Ranjan Kumar

DOI: 10.1504/IJSURFSE.2023.10052346

Article History:
Received: 04 July 2022
Accepted: 27 September 2022
Published online: 08 February 2023

Investigation of solid particle erosion behaviour of Fe-Cr alloy coating

Ratnesh Kumar Sharma

Mechanical Engineering Department,
Poornima College of Engineering,
Jaipur, India
Email: ratnesher@gmail.com

Randip Kumar Das

Mechanical Engineering Department,
IIT (ISM) Dhanbad, India
Email: ranjan.shiv@gmail.com
Email: ranadipda69@gmail.com

Shiv Ranjan Kumar*

Mechanical Engineering Department,
IIMT Engineering College,
Meerut, India
Email: ranjan.shiv@gmail.com
*Corresponding author

Abstract: The purpose of present study was to examine the erosion wear behaviour of Fe-Cr coating deposited on 316 L steel using HVOF coating technology. Chromium content was varied (0–15) wt. % in the step of 5 wt. %. The erosion wear test was performed on Air Jet Erosion Tester by choosing set of parameters as per steady state condition and Taguchi Orthogonal array L16. On adding 5 wt. % Cr, the mechanical properties such as hardness and fracture toughness were improved by 21% and 47% respectively. In steady-state wear conditions, specific wear rate was increased with the increase in impact velocity and slurry concentration. Taguchi design of experiment revealed a particular set of parameter for minimum erosion wear rate such as chromium content of 15 wt. %, impact velocity of 40 m/sec, impingement angle of 45° and slurry concentration of 8 gm/litre.

Keywords: Fe-Cr coating; HVOF coating; chromium; solid particle erosion; SEM image.

Reference to this paper should be made as follows: Sharma, R.K., Das, R.K. and Kumar, S.R. (2023) 'Investigation of solid particle erosion behaviour of Fe-Cr alloy coating', *Int. J. Surface Science and Engineering*, Vol. 17, No. 1, pp.44–57.

Biographical notes: Ratnesh Kumar Sharma has completed his PhD from Mechanical Engineering Department, Indian Institute of Technology (ISM), Dhanbad, India. He is currently working as an Associate Professor in the

Mechanical Engineering Department, Poornima College of Engineering, Jaipur, India. His areas of research are material science, coating techniques and mechanical characterisation.

Randip Kumar Das is a Professor in the Mechanical Engineering Department, Indian Institute of Technology (ISM), Dhanbad, India. His fields of interest are material science and thermal engineering.

Shiv Ranjan Kumar is an Associate Professor in the Department of Mechanical Engineering, IIMT Engineering College, Meerut, India. His fields of interest are composite materials, surface engineering and tribology.

1 Introduction

Surface engineering is one the most widely used method for adding superior properties to the material surface. However, it doesn't have significant effect on the properties of substrate. The performance of material surface is improved by depositing the coating material over the surface. The characteristics of coating is varied by type of coating process, coating thickness, coating layer, etc. In the field of surface engineering, thermal spray coating exhibits promising potential due to economical process, simpler design and easy to use. Thermal spraying process consists of three major phases in which first phase includes melting of material being coated, second phase includes spraying on coating material and in last phase deposition over a substrate in laminate structure (Sampath, 2009). Various kinds of thermal spraying techniques such as arc spraying, plasma spraying, HVOF spraying, HVAF spraying, etc. have been developed and found suitable for many industrial application (Zhou et al., 2009; Sharma et al., 2021a, 2021c, 2020). Arc spray produces cost effective metallic coating for wide range of application. Among all spray coating technique, high-velocity oxygen fuel (HVOF) results into compact and very dense coating (Sidhu et al., 2005). In HVOF, mixture of liquid fuel and oxygen is ignited to produce a hot high-pressure gas stream. The metallic powder which is to be coated over substrate is injected into the gas stream. For coating purpose in metallic substrate in large number of application, Fe-Cr coating has shown much superior physical, mechanical, erosion resistance and corrosion resistance (Nayana et al., 2019; Chu et al., 2020). Solid particle erosion involves continuous impact of solid particle over the coated and uncoated surface (Fu et al., 2021). In order to study the wear behaviour, solid particle erosion wear test is generally performed under varying wear parameters such as impact velocity, impingement angle, particle concentration, etc. The particle size affects the erosion wear in the power law relation (Desale et al., 2009). Also, the erosion wear rate was found proportion to the ratio of hardness of erodent particle and hardness of target surface. It was reported that the major factor influencing erosive wear rate was impact velocity and particle size followed by particle concentration (Avcu et al., 2013). Jha et al. (2011) conducted erosion wear test and revealed that erosive wear rate was increased with the increase in impingement angle. Also, the wear rate was dependent on the abrasive particle concentration. The erosion resistance of hardened high-speed steel was lower than hardened chromium steels (Fernandes et al., 2012). Introduction of chromium as HVOF-spray Cr_2O_3 coated turbine steels improved the erosion wear rate of steel (Oh et al., 1999). In order to sort out the erosion and corrosion issue in boiler and hydraulic turbine, research are being conducted to develop Fe coating with Fe-Cr alloy with superior erosion and corrosion resistance properties. Chromium finds its applications in wide range of field such as tool steel industry, chemical industry, food processing industry, automotive industry, valve parts, turbine blade, pump component, shaft, high temperature corrosion resistance alloy.

Improve in hardenability and corrosion resistance due to addition of chromium is generally presented in the most of the related literature. However, detail study of effect of chromium on erosion wear behaviour is lacking in literature.

Therefore, the aim of present study is to investigate the effect of chromium and erosion wear parameters such as impact velocity, impingement angle, and particle concentration on the erosion wear rate of Fe-Cr alloy coating materials.

2 Materials and Method

2.1 Materials used and HVOF coating deposition

Metallic powder of iron, titanium, chromium, molybdenum, carbon and silicon (in the particle size of 50 = 90 μ) were purchased from local market and used for coating preparation. Four different composition of powder mixture were prepared by varying chromium (0–15 wt. %) in the step of 5 wt. % Table 1. For substrate purpose, 316L steel was used and cleaned before making coating over the surface. High velocity oxy fuel thermal spraying was performed for the deposition of coating material over 316L using HVOF spraying equipment (Hypojet-HP2700, Jodhpur, India).. The coating parameters were kept at spray distance of 200 mm, oxygen flow rate of 300slpm, LPG flow rate of 60 slpm and oxygen pressure of 10 kg/cm^2.

Table 1 Formulation of Fe-Cr coating material

Fe-Cr coating	*Fe (wt. %)*	*Mo (wt. %)*	*C (wt. %)*	*Si (wt. %)*	*Ti (wt. %)*	*Cr (wt. %)*
Fe-Cr-0	60	5	15	10	10	0
Fe-Cr-5	55	5	15	10	10	5
Fe-Cr-10	50	5	15	10	10	10
Fe-Cr-15	45	5	15	10	10	15

2.2 Mechanical and wear testing

The mechanical properties such as hardness, fracture toughness, erosion wear resistance were measured. Instrument used for hardness was Vicker's Hardness Tester (NEXUS 4303, Europe) Indentation was done by applying load of 300gm for 30s. The fracture toughness was also measured using the same hardness tester by creating a crack as per the methodology (Ponton and Rawlings, 1989).

Solid particle erosion test was conducted on Air Jet Erosion Tester (DUCOM Bangalore, India) according to standard of ASTM G-76-13 under varying impact speed, impingement angle and slurry concentration. The varying level of erosion wear parameter were impact speed of 40 m/sec, 60 m/sec, 80 m/sec and 100 m/sec and impingement angle of 45°, 60°, 75°and 90°, slurry concentration of 6 gm/litre, 8 gm/litre, 10 gm/litre and 12 gm/litre (Table 2). The minimum number of experiment to study the effect of varying all parameters was done using Taguchi orthogonal array L16. As compared to other existing design of experiment methods, Taguchi method exhibits the advantages of simple to use, optimisation of numerous factors and finding of qualitative results at less experimental trial (Pundir et al., 2018). Field Emission Scanning electron microscope (NOVA NANOSEM 450, Hillsboro, USA) was used for qualitative understanding of erosion parameter on erosion performance of Fe-Cr alloy coating materials.

Table 2 Levels of variables used in erosion wear rate

Control factors		*LEVEL*				*Unit*
		I	*II*	*III*	*IV*	
A	Chromium content	0	5	10	15	weight%
B	Impact velocity	40	60	80	100	m/sec
C	Impingement angle	45	60	75	90	°
D	Slurry concentration	6	8	10	12	gm./litre

Notes: All experiments were performed under the constant parameter of erodent particle of alumina (80 μm), standoff distance (50 mm), and test duration/cycle (20 min)

3 Results and discussion

3.1 Mechanical properties of Fe-Cr alloy coating materials

The mechanical properties of Fe-Cr alloy coating materials were assessed in terms of micro-hardness and fracture toughness. The micro-hardness of Fe-Cr coating material having Cr content from 0–15 wt. % in the range of 5 wt. % was found to be 400 HV, 485 HV, 578 HV and 690 HV respectively and depicted in Figure 1. Figure 1 shows that on adding 5 wt. % of Cr, micro-hardness was increased by 21%. Therefore, increase in Cr content increased the micro-hardness of coating. Presence of Cr led to formation of hard chromium oxide layer over the surface which protected the surface from erosion and corrosion of substrate materials. This chromium oxide was uniformly dispersed in the other matrix material.

The result is in agreement with the work performed by Wang et al. (2017). They concluded that the increase in chromium content increased the stability of passive film oxide layer of Cr_2O which resulted in erosion and corrosion properties enhancement. Moreover, it was also reported that low content of chromium led to formation of spontaneous passive layer compared to high chromium content which formed stable passive layer (Momen and Farzaneh, 2014).

Fracture toughness of coating was also significantly influenced by addition of chromium content. Fracture can also indicate the brittleness of Fe-Cr alloy coating material. Stress intensity factor (K) is used to measure fracture toughness. Figure 2 depicts the variation of stress intensity factor (K) with respect to Cr content. The stress intensity factor of Fe-Cr alloy coating material with varying chromium content from 0–15 wt. % in the range of 5 weight % was found to be 42 MPa.m1/2, 62 MPa.m1/2, 70 MPa.m1/2 and 83 MPa.m1/2 respectively. Addition of 5 wt. % of chromium increased the fracture toughness by 47%. Increase in fracture toughness with increase in chromium content can be seen in Figure 2 which was attributed to the fact that the formation of chromium oxide layer over the substrate blocked and prevented the propagation and generation of crack in the material. Also, formation of chromium oxide enhanced the interaction between the participating elements. Increase in the fracture toughness with addition of chromium was in line with the literature (Gao et al., 2013) in which it was reported that when chromium entered in Fe alloy, it formed two bond Fe-Cr and Fe-Fe and replaced some of Fe atoms. Fe-Cr bond was stronger than Fe-Fe bond. Therefore, more chromium resulted in stronger bond, hence more energy was required to fracture.

Figure 1 Effect of varying chromium content on micro-hardness of Fe-Cr coating

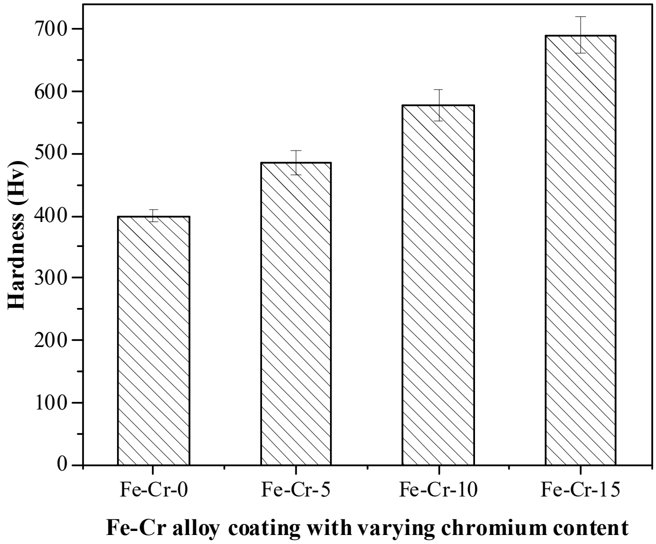

3.2 Steady state wear rate analysis

Solid particle erosion wear rate was evaluated to study the effect of erosion wear parameter. The parameters taken for the study were impact velocity, impingement angle, and slurry concentration.

3.2.1 Effect of impact velocity on the erosion wear rate of Fe-Cr alloy coating materials

The variation of impact velocity on erosion rate was depicted in Figure 3. The impact velocity was varied in the range of 40 m/sec, 60 m/sec, 80 m/sec and 100 m/sec, however, time of impact, impingement angle and slurry concentration of 10 min, 60°, 8 gm/litre respectively were kept constant. It was found that the increase in the impact velocity increased the erosion rate directly. This is in agreement with the fact that there was direct correlation between erosion rate and impact velocity (Salmanzade et al., 2015). Also, it can be seen that increase in chromium content decreased the erosion wear rate. Addition of alloying element such as chromium and titanium increased the hardness and wear resistance (Sharma et al., 2022). Increase in impact velocity increased the kinetic energy of particles and hence resulted into removal of more materials.

Figure 2 Effect of varying chromium content on fracture toughness of Fe-Cr coating

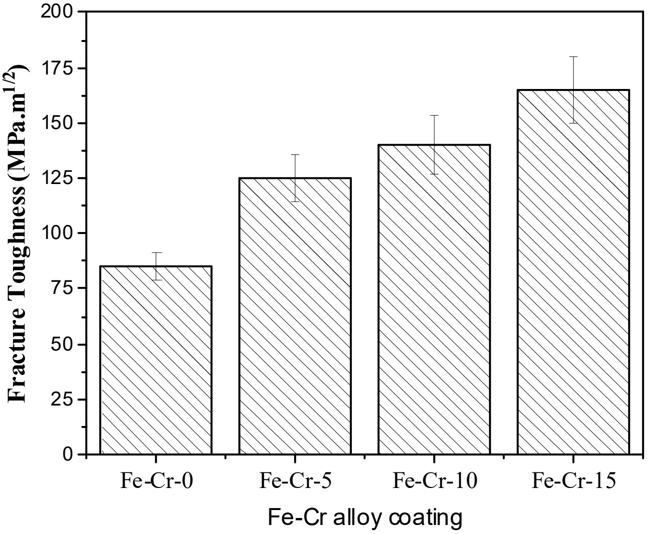

Figure 3 Effect of impact velocity on erosion wear rate of Fe-Cr coating (see online version for colours)

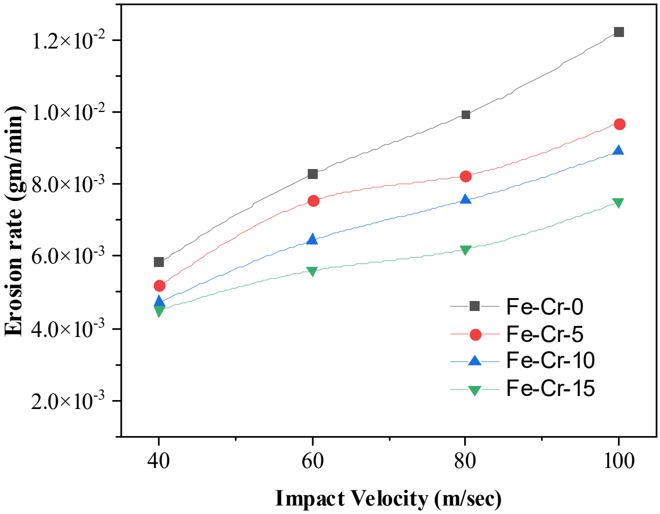

3.2.2 Effect of impingement angle on the erosion wear rate of Fe-Cr alloy coating materials

The variation of impingement angle on erosion rate was depicted in Figure 4. The impingement angle was varied in the range of 45°, 60°, 75° and 90°, however, time of impact, impact velocity and slurry concentration of 10 min, 60 m/sec, 8 gm/litre respectively were kept constant. The impingement angle is the angle between line of impact and horizontal surface. The change in angle changes the mechanism of erosion and influences the erosion rate significantly. It can be seen than the erosion wear rate of coating material was increased when angle of impingement increased from 45° to 75° and later after this angle of 75°, it decreased at 90°. More erosion rate at acute angle of impingement was due to presence of both horizontal and vertical component of forces leading to micro-cutting phenomena. Further, if the variation is analysed step wise, it can be observed that during 45° to 60° of impingement angle, slope of variation in the erosion wear rate is very less as compared to slope of variation in erosion wear rate during 60°–75°. It was due to the fact in case of ductile material, low thrust force was available at lower acute angle and the thrust force increased with the increase in angle of impingement. Erosion rate decreased at 90° due to plastic deformation and absence of shear force.

Figure 4 Effect of impingement angle on erosion wear rate of Fe-Cr coating (see online version for colours)

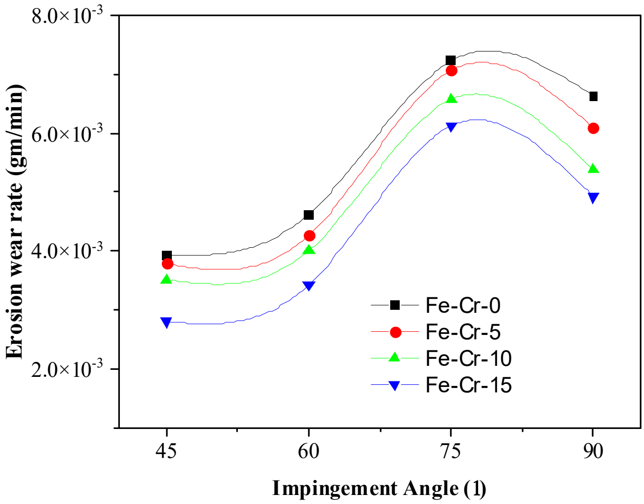

3.2.3 *Effect of slurry concentration on the erosion wear rate of Fe-Cr alloy coating materials*

The variation of slurry concentration on erosion rate was depicted in Figure 5. The slurry concentration was varied in the range of 6 gm/litre, 8 gm/litre, 10 gm/litre, 12 gm/litre, however, time of impact, impact velocity and impingement angle of 10 min, 60m/sec, 60° respectively were kept constant.

It can be seen that the erosion rate was increased with slurry concentration which was obvious. It may attributed to the fact that the increase in the flow rate increased the impact of more particles on the surface resulting into more material deterioration. More deterioration means more ploughing, cutting and plastic deformation. Therefore, more coating material was removed from the surface.

For erosion wear performance, both the mechanical properties micro-hardness and fracture toughness played very important role and have shown different behaviour against varying coating parameter. Increase in the spray distance increased fracture toughness but decrease in the spray distance increased micro-hardness of HVOF coating (Sharma et al., 2021b). In wear test, at high impact velocity, fracture toughness became more significant than micro-hardness of coating.

Figure 5 Effect of slurry concentration on erosion wear rate of Fe-Cr coating (see online version for colours)

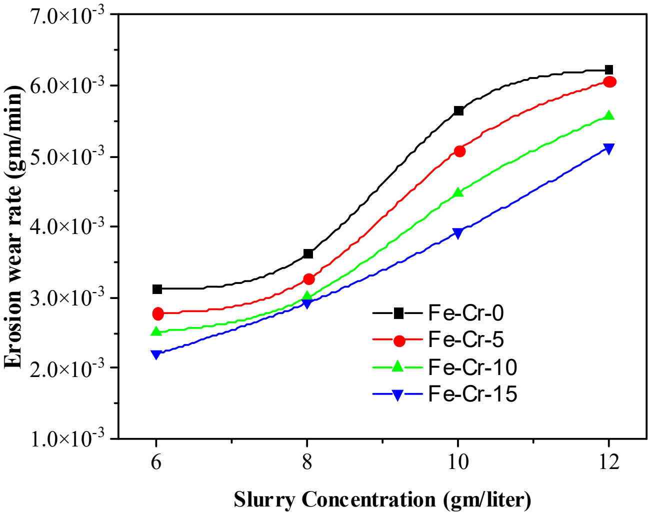

Table 3 Taguchi experimental results

Sl. no.	*Chromium content (%)*	*Impact velocity (m/sec)*	*Impingement angle (°)*	*Slurry concentration (gm./litre)*	*Erosion wear rate (gm/min)*	*S.N ratio (db)*
1	0	40	45	6	0.0043987	47.1334
2	0	60	60	8	0.0055712	45.0809
3	0	80	75	10	0.0068000	43.3498
4	0	100	90	12	0.0085864	41.3238
5	5	40	60	10	0.0049165	46.1669
6	5	60	45	12	0.0051636	45.7410
7	5	80	90	6	0.0059690	44.4820
8	5	100	75	8	0.0067250	43.4462
9	10	40	75	12	0.0039825	47.9969
10	10	60	90	10	0.0043790	47.1725
11	10	80	45	8	0.0046780	46.5988
12	10	100	60	6	0.0058823	44.6091
13	15	40	90	8	0.0022250	53.0534
14	15	60	75	6	0.0029712	50.5412
15	15	80	60	12	0.0035701	48.9463
16	15	100	45	10	0.0038126	48.3757

3.3 Erosion wear rate of experiments performed as per Taguchi Orthogonal array

Taguchi orthogonal array provides the optimum number of experiment to be performed to derive conclusion for different number of factors and levels. The erosion rate obtained after the experiment as per Taguchi method was presented in Table 3. In Table 3, erosion wear rate was shown in column 5 and S/N ratio was shown in column 6. MINITAB 16 was used to analyse the role of each factor on the erosion wear rate. The analysis diagram based on S/N ratio is depicted in Figure 6. Figure 6 showed the effect of control factor on erosion wear rate. It was observed that the best combination of factor influencing the minimum erosion rate was Chromium content of 15 wt. %, (A4), impact velocity of 40 m/sec (B1), impingement angle of 45° (C1) and slurry concentration of 8 gm/litre (B2).

3.4 ANOVA analysis

ANOVA was performed for the qualitative evaluation of each parameter on erosion wear rate. On the basis of response of Taguchi experiments, ANOVA was evaluated under the significance level of 95% and presented in Table 5. The last column of Table 5 indicated the level of significance. After ANOVA, it can be seen that the most influencing factor on erosion wear rate is chromium content (p = 0.001), followed by impact velocity (p = 0.004), slurry concentration (0.167) and impingement angle (0.320). Therefore, addition of chromium played the most significant role in the improvement in mechanical and erosion wear properties. It was already reported that erosion wear rate of ductile materials was more dependent upon impact velocity as compared to slurry concentration (Molina et al., 2021).

Figure 6 Effect of control factors on the erosion wear rate of Fe-Cr coating (see online version for colours)

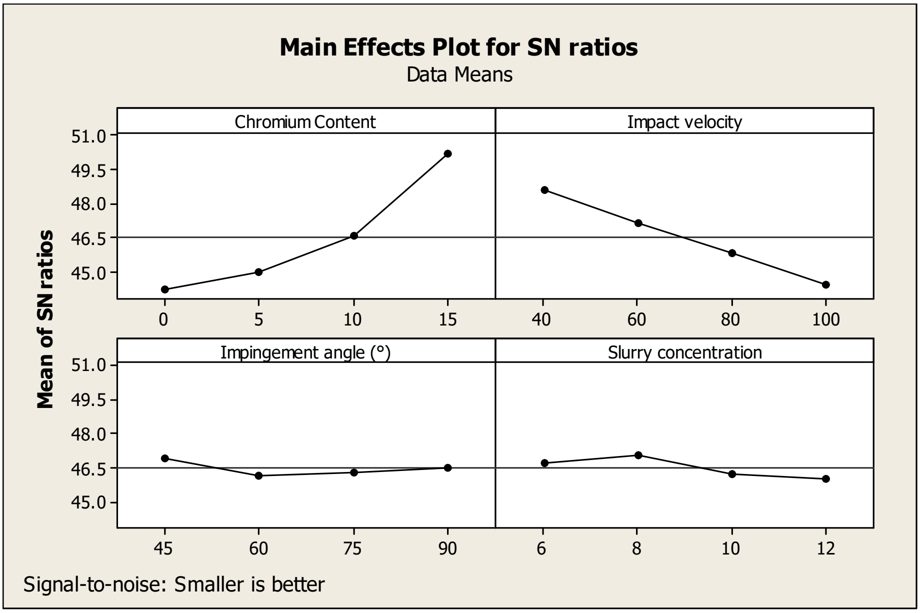

Table 4 ANOVA analysis for volumetric wear rate

Source	*DF*	*Seq. SS*	*Adj. SS*	*Adj. MS*	*F*	*P*
Chromium content	3	85.918	85.918	28.639	117.13	0.001
Impact velocity	3	37.758	37.758	12.586	51.47	0.004
Impingement angle	3	1.324	1.324	0.441	1.80	0.320
Slurry concentration	3	2.545	2.545	0.848	3.47	0.167
Error	3	0.734	0.734	0.245		
Total	15	128.278				

3.5 Microstructure analysis of the steady state erosion wear

3.5.1 Microstructure analysis of steady state erosion test performed by varying impact velocities

Microstructural analysis was conducted for qualitative evaluation of worn surfaces of Fe-Cr coating under the steady state condition of varying impact velocity under constant other parameters. Figure 7 showed the micrograph of worn surface of Fe-Cr alloy under impact velocity of 40m/sec [Figure 7(a)], impact velocity of 60 m/sec [Figure 7(b)], impact velocity of 80m/sec [Figure 7(c)] and impact velocity of 100 m/sec [Figure 7(d)]. At lower velocity, surface showed less erosion wear, crack, void and depth/impact of crater or pit created was less [Figure 7(a)]. As velocity increased, crack started to propagate [Figure 7(b)] and became severe [Figure 7(c)] and finally led to delamination and extensive crater formation [Figure 7(d)]. As in Figure 7(b), increase in impact velocity showed the presence of wear scars. Further increase in speed led to more erosion and hence, some eroded particles were visible [Figure 7(c)]. Finally, at maximum impact velocity [Figure 7(d)], extensive plastic deformation led to formation of deep crater and platelet.

Figure 7 SEM images of Fe-Cr-15 coating for varying impact velocity at, (a) 40 m/sec (b) 60 m/sec (c) 80 m/sec and (d) 100 m/sec

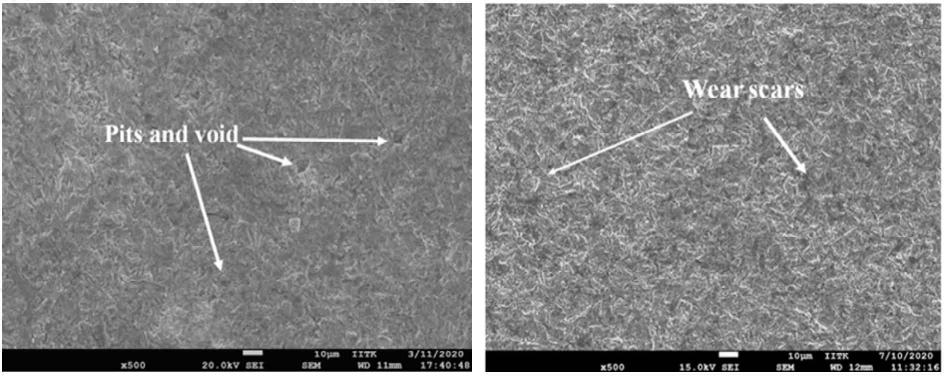

(a) (b)

Figure 7 SEM images of Fe-Cr-15 coating for varying impact velocity at, (a) 40 m/sec (b) 60 m/sec (c) 80 m/sec and (d) 100 m/sec (continued)

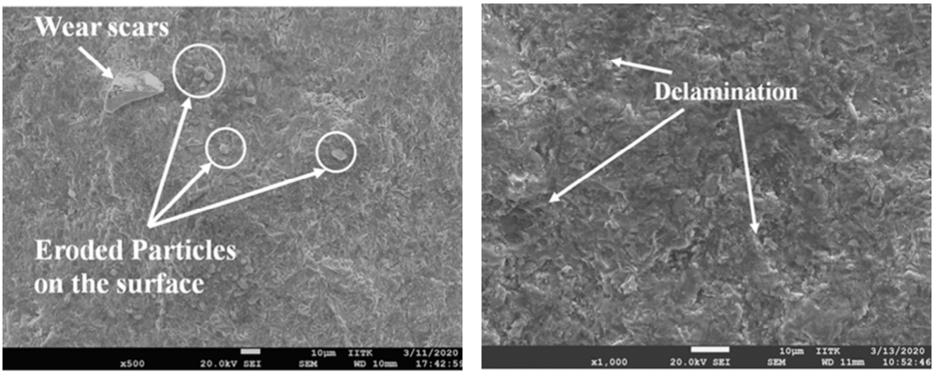

(c) (d)

Figure 8 SEM images of Fe-Cr-15 coating for varying impingement angle at (a) 45° (b) 60° (c) 75° and (d) 90°

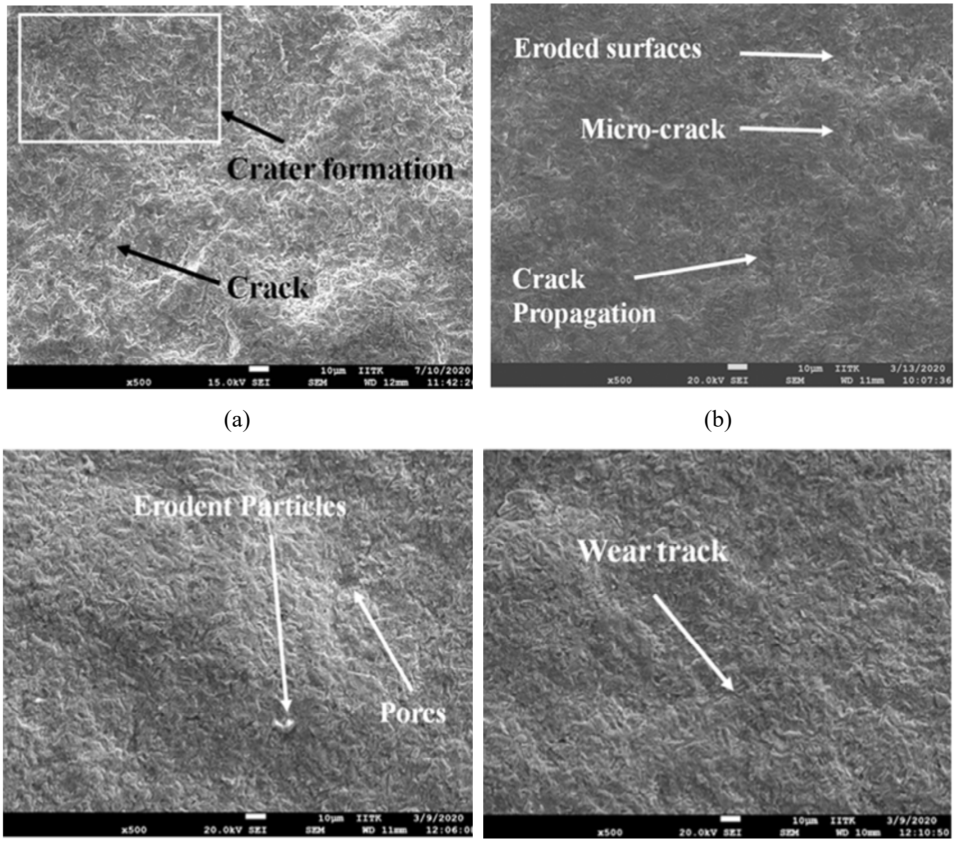

(a) (b)

(c) (d)

3.5.2 Microstructure analysis of steady state erosion test performed by varying impingement angle

Microstructural analysis was conducted for qualitative evaluation of worn surfaces of Fe-Cr coating under the steady state condition of varying impingement angle under constant other parameters. Figure 8 showed the micrograph of worn surface of Fe-Cr alloy under impingement angle of 45° [Figure 8(a)], impingement angle of 60° [Figure 8(b)], impingement angle of 75° [Figure 8(c)] and impingement angle of 90° [Figure 8(d)]. As angle increased in the acute region, i.e., below 90°, both horizontal and vertical component of impact force acted. However, impact of vertical component was more in plastic deformation as micro-cutting mode whereas horizontal force resulted into micro-ploughing which resulted into presence of ploughing area with some removed particle. This phenomena was confirmed from [Figure 8(a), Figure 8(b) and Figure 8(c)]. At impingement angle of 60°, micro crack was generated due to horizontal component. Micro-crack and crater formation was more at 75° [Figure 8(c)]. At impingement angle of 90°, less wear was seen due to absence of horizontal component of impact force [Figure 8(d)].

Figure 9 SEM images of fe-cr-15 coating for varying slurry concentration at, (a) 6 gm/lire (b) 8 gm/litre (c) 10 gm/litre and (d) 12 gm/litre

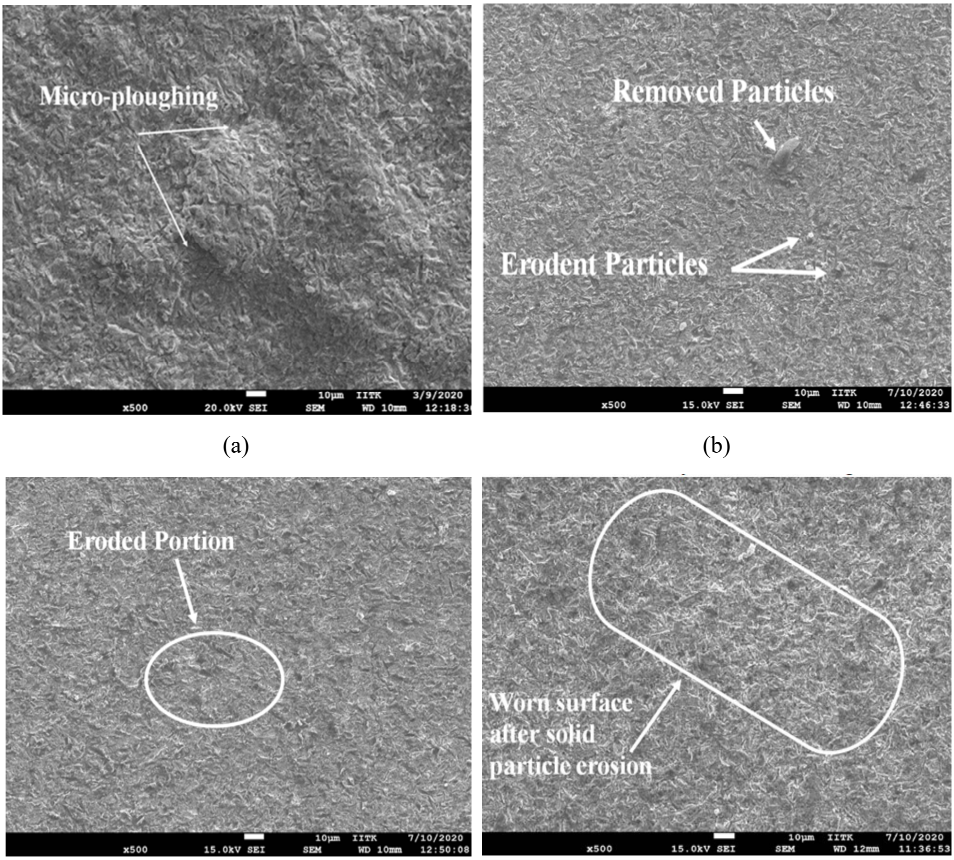

(a) (b)

(c) (d)

3.5.3 Microstructure analysis of steady state erosion test performed by varying slurry concentration

Microstructural analysis was conducted for qualitative evaluation of worn surfaces of Fe-Cr coating under the steady state condition of varying slurry concentration under constant other parameters. Figure 9 showed the micrograph of worn surface of Fe-Cr alloy under slurry concentration of 6 gm/litre [Figure 9(a)], slurry concentration of 8 gm/litre [Figure 9(b)], slurry concentration of 10 gm/litre [Figure 9(c)] and slurry concentration of 12 gm/litre [Figure 9(d)]. Increase in slurry concentration increased the number of particle striking at a time so, more impact on surface resulted into more erosion rate. At lower slurry concentration [Figure 9(a)], micro-ploughing was less so erosion was less but still cracks, pits and voids are present on the worn surface. As slurry concentration was increased to 8 gm/litre [Figure 9(b)], micro-ploughing was increased indicating crater formation which became extensive and deep crater under the slurry concentration of 10 gm/litre [Figure 9(c)]. Figure 9(d) showed interlayer delamination due to increase in the ploughing effect to the maximum extent.

4 Conclusions

HVOF was used to deposit Fe-Cr alloy coating with varying Cr content. Wear properties were evaluated as per steady state condition and Taguchi orthogonal array design of experiments. The mechanical properties such as hardness and fracture toughness were improved by 21% and 47% respectively on adding 5 wt. % Cr. The design of experiment revealed a particular set of parameter for minimum erosion wear rate such as chromium content of 15 wt. %, impact velocity of 40 m/sec, impingement angle of 30° and slurry concentration of 8 gm/litre. ANOVA analysis of Taguchi experiment indicated that chromium and impact velocity have shown significant contribution followed by impingement angle, slurry concentration.

References

Avcu, E., Fidan, S., Yıldıran, Y. and Sınmazçelik, T. (2013) ‘Solid particle erosion behaviour of Ti6Al4V alloy’, *Tribol. – Mater. Surf. Interfaces*, Vol. 2013, No. 7, pp.201–210.

Chu, Z., Deng, W., Zheng, X., Zhou, Y., Zhang, C., Xu, J. and Gao, L. (2020) ‘Corrosion mechanism of plasma-sprayed fe-based amorphous coatings with high corrosion resistance’, *J. Therm. Spray Technol.*, Vol. 29, No. 6, pp.1111–1118.

Desale, G.R., Gandhi, B.K. and Jain, S.C. (2009) ‘‘Particle size effects on the slurry erosion of aluminium alloy (AA 6063)’, *Wear*, Vol. 266, Nos. 11–12, pp.1066–1071.

Fernandes, F.A.P., Heck, S.C., Picon, C.A., Totten, G.E. and Casteletti, L.C. (2012;) ‘Wear and corrosion resistance of pack chromised carbon steel’, *Surf Eng.,* Vol. 8, pp.313–317.

Fu, F., Zhang, Y., Xie, Y., Lu, Y., Sun, J. and Yue, C. (2021) ‘The tribology and erosion-corrosion resistance properties of Fe-Cr-Ni-Si and WC alloy coating’, *Integrated Ferroelectrics*, Vol. 219, No. 1, pp.69–75.

Gao, Y., Lv, Z., Sun, S., Qu, M., Shi, Z., Zhang, R. and Fu, W. (2013) ‘First principles study on surface structure and stability of alloyed cementite doped with Cr’, *Mater. Lett.*, Vol. 100, pp.170–172.

Jha, A.K., Batham, R., Ahmed, M., Majumder, A.K., Modi, O., Chaturvedi, P.S. and Gupta, A.K. (2011) 'Effect of impinging angle and rotating speed on erosion behavior of aluminum', *T. Nonferr. Metal. Soc.*, Vol. 21, pp.32–38.

Molina, N., Walczak, M., Kalbarczyk, M. and Celentano, D. (2021) 'Erosion under turbulent slurry flow: Effect of particle size in determining impact velocity and wear correlation by inverse analysis', *Wear*, Vol. 299, pp.474–475.

Momen, G. and Farzaneh, M. (2014) 'Facile approach in the development of icephobic hierarchically textured coatings as corrosion barrier', *Appl. Surf. Sci.*, Vol. 299, pp.41–46.

Nayana, K.O., Prashanth, S.A., Venkatesha, T.V. and Pandurangappa, M. (2019) 'Effect of additives on nanocrystalline bright Zn–Ni–Fe alloy electrodeposit properties', *Surf Eng.*, Vol. 35, No. 12, pp.1061–9.

Oh, Y., Ryu, W., Sung, C., Kuk, I. and Hong, J. (1999) 'Grain boundary film like Fe–Mo–Cr phase in nitrogen-added type 316L stainless steels', *J. Mater. Res.*, Vol. 14, pp.390–397.

Ponton, C.B. and Rawlings, R.D. (1989) 'Vickers indentation fracture toughness test Part 1 Review of literature and formulation of standardised indentation toughness equations', *Mater Sci. Technol.,* Vol. 5, pp.865–872.

Pundir, R., Chary, G.H.V.C. and Dastidar, M.G. (2018) 'Application of Taguchi method for optimizing the process parameters for the removal of copper and nickel by growing Aspergillus sp', *Water Resources and Industry*, Vol. 20, pp.83–92.

Salmanzade, M., Azizpour, M.J. and Majd, H.M. (2015) 'Evaluation of the effect of spray distance on fracture toughness of thermally sprayed coatings', *J. of Applied Sciences*, Vol. 15, No. 4, pp.709–714.

Sampath, S. (2009) 'Thermal sprayed ceramic coatings: fundamental issues and application considerations', *IJMPT*, Vol. 35, Nos. 3/4, pp.425–448.

Sharma, R.K., Das, R.K. and Kumar, S.R. (2020) 'Microstructure, adhesion and erosion properties of Fe-Cr-Ti-Mo-C-Si coating with varying Titanium', *Mater. Today Commun.*, Vol. 26, p.101826.

Sharma, R.K., Das, R.K. and Kumar, S.R. (2021a) 'Effect of chromium content on microstructure, mechanical and erosion properties of Fe-Cr-Ti-Mo-C-Si coating', *Surf. Interfaces*, Vol. 22, p.100820.

Sharma, R.K., Das, R.K. and Kumar, S.R. (2021b) 'Effect of HVOF spraying parameters on fracture, erosion and thermal properties of Fe alloy-based coating materials', *Proc. Inst. Mech. Eng. L. P. I MECH ENG L-J MAT.,* Vol. 235, No. 7, pp.1703–1711.

Sharma, R.K., Das, R.K. and Kumar, S.R. (2021c) 'Microstructure, mechanical and erosion wear analysis of post heat treated iron alloy based coating with varying chromium', *Materialwiss Werkstofftech*, Vol. 52, No. 11, pp.1173–1184.

Sharma, R.K., Das, R.K. and Kumar, S.R. (2022) 'Effect of chromium–titanium on corrosion and erosion of HVOF coating', *Surface Engineering,* Vol. 38, No. 4, pp.366–374.

Sidhu, T.S., Prakash, S. and Agrawal, R.D. (2005) 'State of the Art of HVOF coating investigations–a review', *Mar. Technol. Soc. J.,* Vol. 39, No. 2, pp.53–64.

Wang, Y., Li, C. and Lin, Y. (2017) 'Electronic theoretical study of the influence of Cr on corrosion resistance of Fe-Cr Alloy', *Acta. Metall. Sin.*, Vol. 2017, No. 53, pp.622–630.

Zhou, Z., Wang, L., Wang, F.C., Zhang, H.F., Liu, Y.B. and Xu, S.H. (2009) 'Formation and corrosion behavior of Fe-based amorphous metallic coatings by HVOF thermal spraying', *Surf Coat Technol.*, Vol. 204, No. 5, pp.563–570.